

# Fluorescence Behavior of Polymer Liquid Crystals with Mesogenic Cyanobiphenyl Side Chains

Seiji Kurihara, Tomiki Ikeda,\* and Shigeo Tazuke†

Research Laboratory of Resources Utilization, Tokyo Institute of Technology,  
4259 Nagatsuta, Midori-ku, Yokohama 227, Japan

Received September 14, 1992; Revised Manuscript Received December 9, 1992

**ABSTRACT:** The role of the ground-state morphology on excimer formation has been explored for five kinds of polymer liquid crystals (PLCs) with mesogenic cyanobiphenyl side chains through various alkyl spacers. The PLCs studied here are poly[(4-cyanobiphenyl)-4'-oxyalkyl acrylate] (PACB $n$ ), in which the alkyl spacer (CH $_2$ ) $_n$  was varied as  $n = 2, 3, 5, 6$ , and  $11$ . In PLCs with a short alkyl spacer such as PACB2 and PACB3, excimer formation is depressed in the neat film in comparison with PACB5 and PACB6. This may be explicable by the strong coupling of the mesogenic moieties with the main chain, which results in a lower mobility of the cyanobiphenyl moieties. PACB11 showing a smectic phase also exhibited the depression of excimer formation. In this case, diffusion of the cyanobiphenyl moieties is highly suppressed owing to the restricted mobility of mesogens in the smectic phase.

## Introduction

In polymer liquid crystals (PLCs) with mesogenic side chains, only the side-chain mesogens are responsible for the liquid-crystalline order. The order is considered to be more or less independent of the conformation of the polymer main chain. Therefore, it is assumed that side-chain PLCs are very similar to conventional low-molecular-weight liquid crystals (LMWLCs) in the manner of the liquid-crystalline phase formation.<sup>1</sup> However, the interesting properties of PLCs, which arise from a cooperative interaction among mesogens, depend not only on the structures of the main chain and spacers but also on molecular weight, molecular weight distribution, and tacticity. The effect of the alkyl spacer on the morphology of the liquid-crystalline state was investigated for PLCs with a smectic phase,<sup>2,3</sup> and the mesogenic ordering was explored for PLCs with a nematic phase.<sup>4</sup>

Fluorescence probes are useful for the investigation of microscopic environments owing to the rich information associated with this method. The fluorescence is quite sensitive to the microenvironment around the fluorophore, so that a variety of information can be obtained by steady-state as well as time-resolved fluorescence measurements.<sup>5,6</sup> Usually a fluorophore is incorporated as a *probe* into the system just by doping or by covalent attachment, and we can obtain information on the microscopic environment around the probe. Thus, the location of the probe is of primary importance. However, it is not easy to control the location of the probe. Also, we have to consider the perturbation due to the incorporation of the probe into the system. This is always a problem as long as *extrinsic* probes are used. To avoid perturbation by foreign labels, one should use *intrinsic* probes, but few chromophores are available for *intrinsic* probes which satisfy conditions such as high fluorescence quantum yield, high photochemical stability, and clear photophysical properties.<sup>7</sup>

The cyanobiphenyl (CB) moiety is a common mesogen, and many LC materials which contain the CB moiety have been employed in display devices. The CB moiety is also well-known as an emissive mesogen, and studies on its photophysical properties have been reported.<sup>8-10</sup> It is, therefore, expected that we will be able to obtain much information on the microscopic environment in the LC

phase with the aid of CB mesogens as *intrinsic* probes. In addition, the CB mesogens form excimers, so we can obtain additional information on orientational ordering.<sup>8-10</sup> In this respect, the kinetic behavior of excimer formation in the CB mesogens has been extensively investigated by Subramanian et al.,<sup>8</sup> Yamazaki et al.,<sup>9</sup> and us.<sup>10</sup> In this paper, we explored the fluorescence behavior of the CB mesogens covalently attached to the side chains of polyacrylates by steady-state and time-resolved fluorescence spectroscopy and discuss the orientational ordering of the CB mesogens in the side-chain PLCs on the basis of those results.

## Experimental Section

**Materials.** The structure of PLCs used in this study is shown in Figure 1. Polyacrylates with mesogenic cyanobiphenyls (CBs) in the side chain (PACB $n$ ) were prepared by the method reported by Shibaev et al.<sup>11</sup> Polymerization was conducted in tetrahydrofuran (THF) using azobis(isobutyronitrile) (AIBN) as initiator. All polymers were purified by reprecipitation from chloroform solution into methanol. 4-(*n*-Pentyloxy)-4'-cyanobiphenyl (5OCB) was purchased from Merck Co. and was used without further purification.

**Characterization of Polymers.** The thermodynamic data of PLCs are indicated in Table I. The molecular weight (MW) of the polymers was determined by gel permeation chromatography (GPC; Tosoh HLC-802, column, GMH6  $\times$  2 + G4000H8 + G2500H8; eluent, chloroform) calibrated with standard polystyrenes. Liquid-crystalline behavior and phase-transition behavior were examined on an Olympus Model BHSP polarizing microscope equipped with Mettler hot stage Models FP-80 and FP-82. Thermotropic properties and glass transition temperatures ( $T_g$ ) were determined with a differential scanning calorimeter (DSC; Seiko I&E SSC-5000) at a heating rate of 10 °C/min. At least four scans were performed for each sample to check reproducibility.

**Sample Preparation.** Sample solutions for the spectroscopic measurements were prepared by degassing the THF (spectroscopic grade) solutions of PACB $n$  or 5OCB in quartz cells by several freeze-pump-thaw cycles. PACB $n$  films were prepared by casting the PLC solution in a quartz cell (10  $\times$  10  $\times$  40 mm) which had been placed horizontally, followed by gradual evaporation of the solvent under a nitrogen stream and subsequently under reduced pressure. The films were then kept under vacuum for several days, and the cell was sealed. In this way, the PLC films adhering to the inner surface of one plane of the cell were prepared, which enabled the spectroscopic measurements of the PLC films in the absence of air.

**Measurements.** Steady-state fluorescence spectra (corrected) were measured on a Hitachi F-4000 fluorescence spectrometer.

\* Author to whom correspondence should be addressed.

† Deceased July 11, 1989.

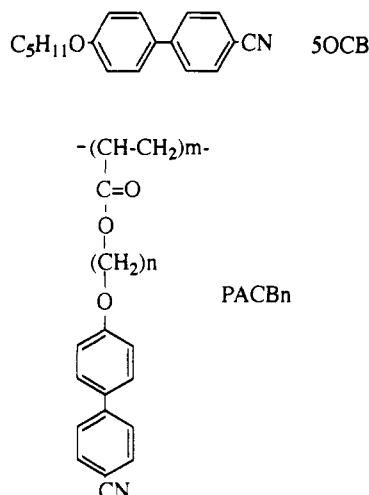


Figure 1. Structures of PACBn and 5OCB.

Table I  
Thermodynamic Properties of PACBn

<i>n</i>	<i>M<sub>n</sub></i>	<i>T<sub>c</sub></i> , °C	<i>T<sub>g</sub></i> , °C	$\Delta H$ , J/mol	$\Delta S$ , J/mol·K
2	3800	98	66	322	0.87
3	4200	72	48	31	0.09
5	4600	77	42	100	0.28
6	4800	104	24	800	2.12
11	5000	115	5	3300	8.51

Time-resolved fluorescence measurements were performed with a picosecond time-correlated single-photon counting system as reported elsewhere.<sup>12</sup> The instrument response function of the system was 60-ps fwhm. The spectra were not corrected for the wavelength-dependent sensitivity of the photomultiplier used in our system (Hamamatsu R1564U-01).

Fluorescence spectra of PACBn in the neat were observed by front-face excitation and front-face measurement of emission. The temperature was controlled by a Jasco HTV cell coupled with a temperature-controlling unit.

## Results and Discussion

**Fluorescence Behavior in Solution.** Figure 2 shows fluorescence and absorption spectra of PACBn and 5OCB in THF. In a dilute solution ( $3 \times 10^{-6}$  M) of PACB3, the fluorescence spectrum had a maximum at 368 nm, which was broad in the longer wavelength region compared to that of 5OCB, while the absorption spectrum of PACB3 was approximately identical to that of 5OCB (Figure 2A). The emission in the longer wavelength region in PACB3 could be assigned as excimer emission.<sup>8-10</sup> The emission spectra depended on the alkyl spacer length as shown in Figure 2B, in which the fluorescence spectra of PACBn were normalized at the maximum wavelength, assigned as the peaks of monomer emission. In solution, the efficiency of excimer formation, evaluated by the fluorescence intensity at 450 nm in the normalized spectra, increased in the order of PACB11 < PACB2 < PACB5 ~ PACB6 < PACB3. The CB chromophores of PACB11 are effectively isolated from each other due to the decoupling of the CB moieties from the main chain, leading to a low efficiency of the excimer formation. On the other hand, the CB mesogens in PACB3 have a favorable distribution for the face-to-face configuration, essential for the excimer formation, and the reorientation process of the two relevant chromophores, also necessary for the excimer formation, is easily attainable with the aid of the solvent molecules, which results in a high efficiency of the excimer formation. In PACB2 with a shorter methylene spacer, the CB mesogens are expected to be strongly coupled with the main chain so that the efficiency of the excimer formation decreases due to suppression of the mobility of the CB mesogens. This sort of restricted motion of the side-chain

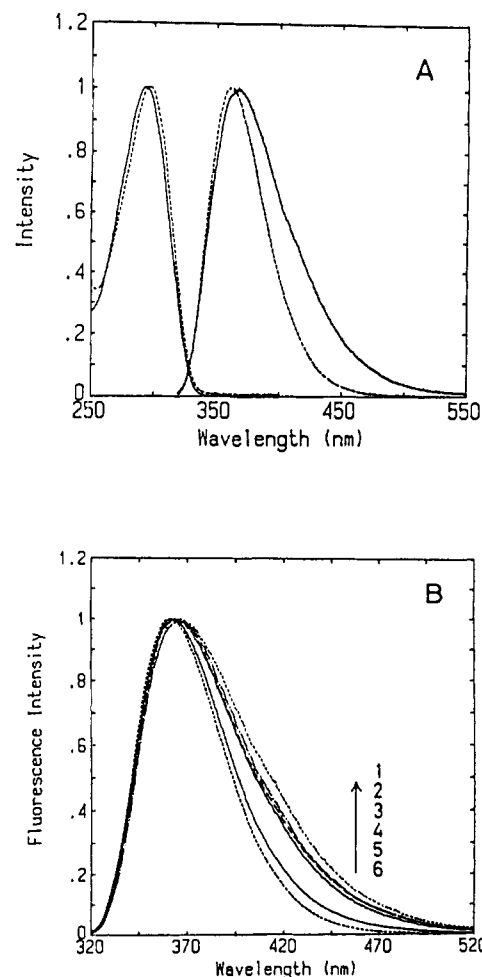
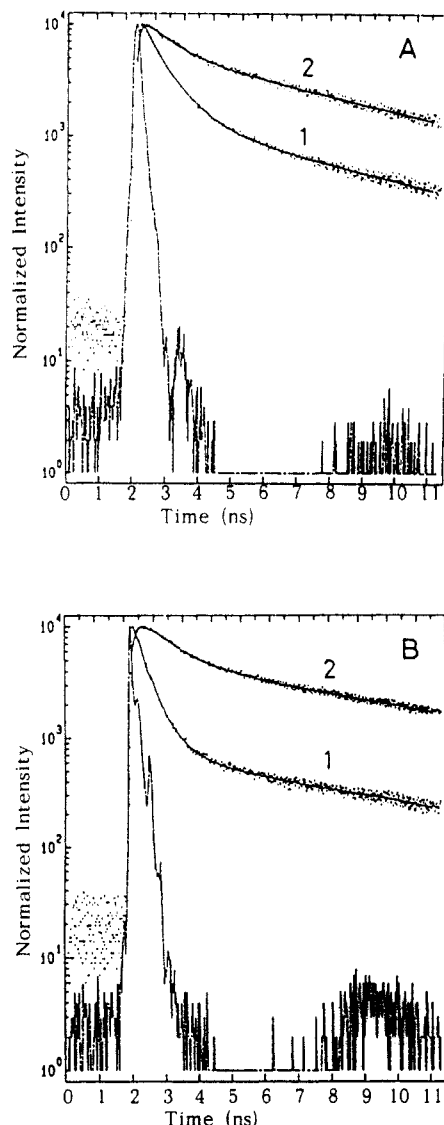


Figure 2. Absorption and fluorescence spectra (normalized) of PACB3 (—) and 5OCB (···) in THF (A) and fluorescence spectra of PACBn in THF (B). Excitation was at 300 nm. 1, PACB3; 2, PACB6; 3, PACB5; 4, PACB2; 5, PACB11; 6, 5OCB.

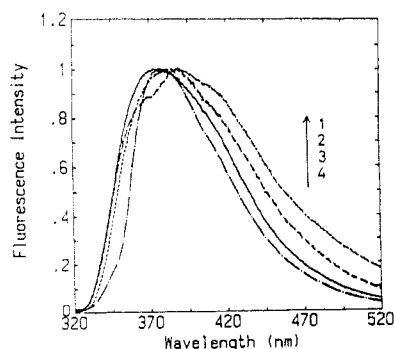
chromophores has already been reported for naphthalene moieties attached to the polymer main chain through alkyl spacers such as poly(1-naphthylmethyl methacrylate) and poly(1-naphthylethyl methacrylate). The intensity of the excimer emission was found to decrease with the spacer length.<sup>13</sup>

Figure 3A shows typical examples of the decay profiles of the monomer emission monitored at 367 nm and of the excimer emission monitored at 450 nm in dilute solution ( $3 \times 10^{-6}$  M) at room temperature (24 °C). Both the monomer and the excimer emissions of PACBn in dilute solutions could be analyzed by the triple-exponential function in the form of  $A_1 \exp(-t/\tau_1) + A_2 \exp(-t/\tau_2) + A_3 \exp(-t/\tau_3)$  as judged by reduced  $\chi^2$  and Durbin-Watson (DW) parameters. A double-exponential function was examined but gave a poorer fitting. The monomer emissions were associated with fast-decaying components ( $\tau_1 = 50$ –100 ps), components with lifetimes  $\tau_2$  of 700–1100 ps, and slowly-decaying components ( $\tau_3 = 5$ –6 ns). It is noted that no rising component was observed for all PACBn ( $n = 2, 3, 5, 6$ , and 11) in dilute solutions. This seems to indicate that the excimer formation in the dilute solutions is too fast to be detectable with our apparatus. In the excimer emissions components were observed with lifetimes  $\tau_1$  of 50–100 ps,  $\tau_2$  of 400–1000 ps, and  $\tau_3$  of 4–6 ns.

The emission spectra of concentrated solutions of PACBn (1 M in THF) are shown in Figure 4. In the concentrated solutions of PACBn, spectra were observed with maxima at longer wavelength than those of the dilute solutions. This is probably due to the much larger



**Figure 3.** Decay profiles of dilute (A) and concentrated (B) solutions of PACB3 in THF at 24 and 21 °C, respectively. Excitation was at 310 nm. (A)  $3 \times 10^{-6}$  M; (B) 1 M. 1, monitored at 367 nm; 2, monitored at 450 nm.



**Figure 4.** Fluorescence spectra (normalized) of a concentrated solution of PACBn in THF. Excitation was at 300 nm. 1, PACB3; 2, PACB5; 3, PACB2; 4, PACB11.

contribution of the excimer to the total emission in the concentrated solutions. In dilute solutions, *intramolecular* excimer formation of the CB chromophores may be predominant, but in the concentrated solutions *intermolecular* excimer formation contributes and leads to the red-shifted emission spectra. Dependence upon the length of the alkyl spacer was also observed. For the concentrated solutions, the decay profiles of the monomer emission monitored at 367 nm and of the excimer emission monitored at 21 °C are also included in Figure 3B. Both

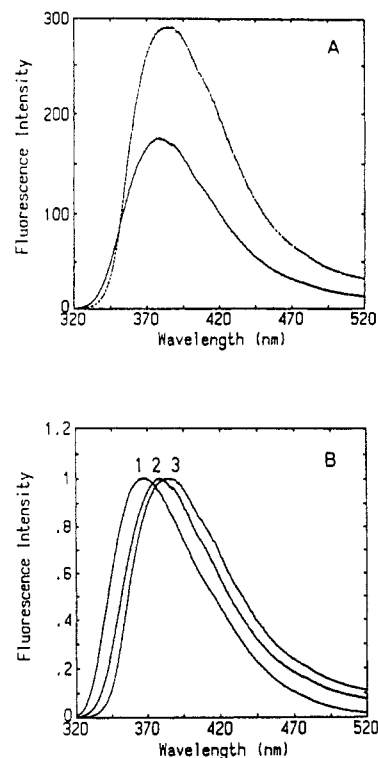


**Figure 5.** Fluorescence spectra of neat PACB3 in the I state (—; 143 °C) and the N state (···; 61 °C) (A) and normalized fluorescence spectra of PACB3 in various phases (B). 1, in THF; 2, I state; 3, N state.

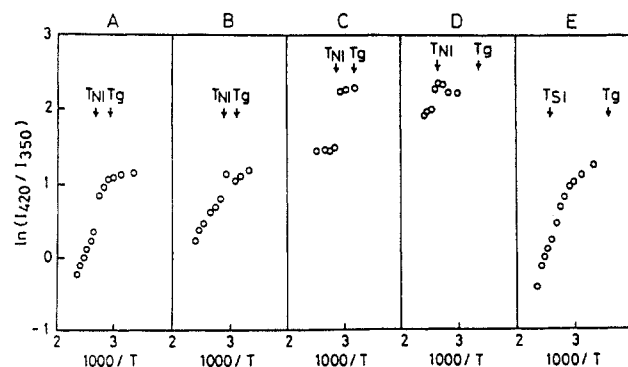


**Figure 6.** Arrhenius plots for a fluorescence intensity ratio of  $I_D/I_M$  in the neat film of PACBn: A, PACB2; B, PACB3; C, PACB5; D, PACB6; E, PACB11.  $I_D$  and  $I_M$  are the fluorescence intensities of excimer (450 nm) and monomer (360 nm), respectively.

the monomer and excimer emissions were again analyzed by the triple-exponential function as for the dilute solutions. The monomer emissions were associated with fast-decaying components ( $\tau_1 = 100$ –200 ps), components with lifetimes  $\tau_2$  of 500–600 ps, and slowly-decaying components ( $\tau_3 = 6$ –7 ns). Contrary to the results of the dilute solutions, a rising portion was observed in the excimer emissions. These comprised the rising components with lifetimes  $\tau_1$  of 10–50 ps,  $\tau_2$  of 800–1500 ps, and  $\tau_3$  of 7–10 ns.

**Fluorescence Behavior in Neat PACBn.** Figure 5A shows the fluorescence spectra of neat PACB3 in the isotropic (I) and nematic (N) phases. The fluorescence intensity of the N state is higher than that of the I state, and at the same time the emission is slightly red-shifted in the N state. In Figure 5B, the fluorescence spectra of PACB3 in various phases are shown.

As a measure of efficiency for the excimer formation, the ratio of the fluorescence intensity at 450 nm (excimer fluorescence,  $I_D$ ) to that of 362 nm (monomer fluorescence,  $I_M$ ),  $I_D/I_M$ , was determined. In Figure 6  $I_D/I_M$  is plotted

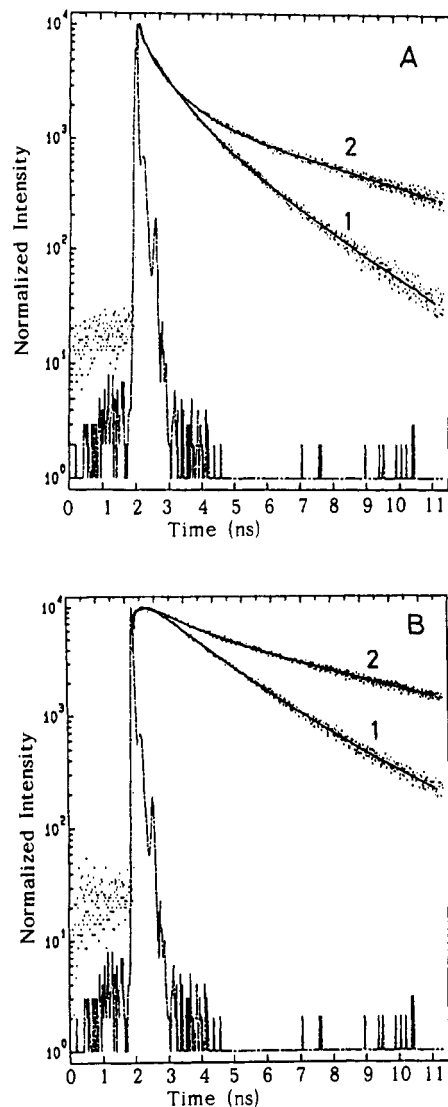


**Figure 7.** Decay profiles of monomer (A) and excimer (B) of neat PACB3 in the I state (165 °C; curve 1) and N state (50 °C; curve 2). Excitation was at 310 nm. A, monitored at 363 nm; B, monitored at 450 nm.

for PACB $n$  as a function of the reciprocal of the absolute temperature. Data were observed during cooling. In all samples the excimer is formed with a high efficiency in the N state, and an abrupt change in the ratio of  $I_D/I_M$  is observed at a temperature close to the N-I phase transition temperature ( $T_{NI}$ ) indicated by arrows in the figure. These results indicate that the morphology of the LC state affects the excimer formation as observed in the LMWLC systems.<sup>10</sup> In the N state, mesogens are aligned parallel to each other, so that the face-to-face conformation necessary for the excimer formation is easily attained with only a small reorientation of the CB mesogens. On the other hand, in the I state, the mesogens are randomly oriented, and a large movement is required for the CB mesogens to take the face-to-face configuration. In addition, a strong tendency of CB mesogens to associate in the ground state to form a head-to-tail pair<sup>14</sup> is also expected to enhance the excimer formation in the N state. It is noted that continuous change in the values of the  $I_D/I_M$  ratio was observed on the phase transition of PACB11 showing a smectic A ( $S_A$ ) phase.

In Figure 7, two decay curves are shown for the neat film of PACB $n$ : the monomer (monitored at 363 nm) and the excimer emissions (monitored at 450 nm) of the PACB3 film, representative of the N state (50 °C) and the I state (165 °C). Both the monomer and excimer emissions in all the PLCs could be analyzed by the triple-exponential

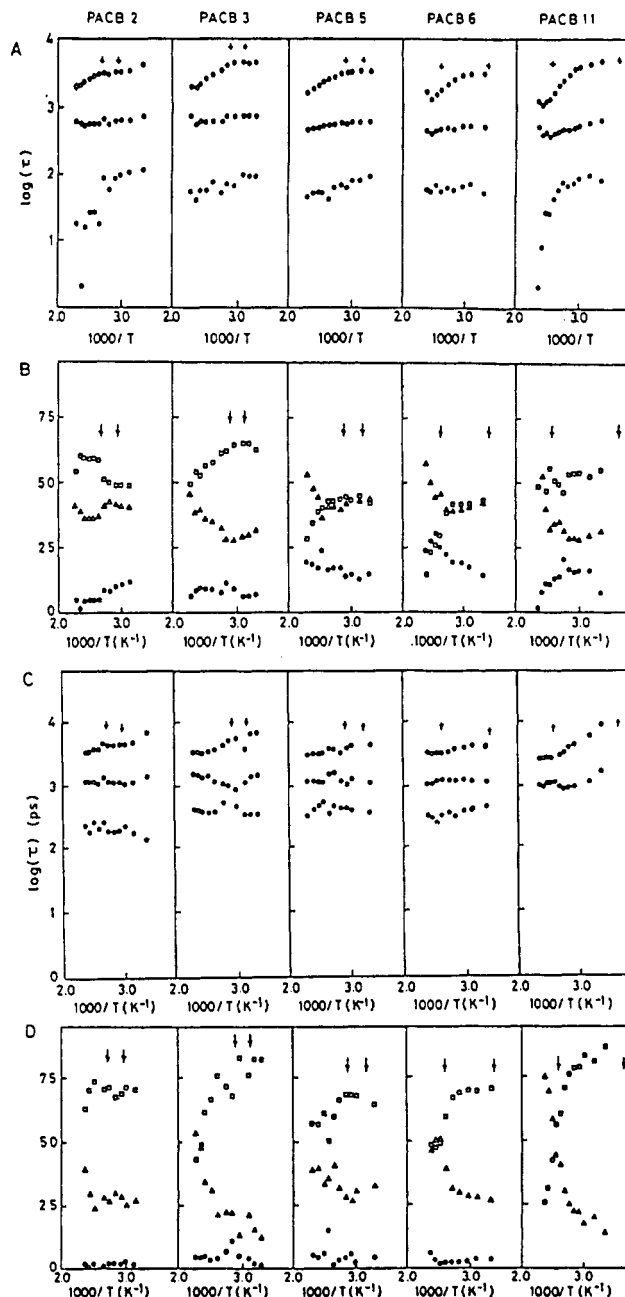


**Figure 8.** Lifetimes (A and C) and the fraction of each component (B and D) of excimer and monomer emissions. Excitation was at 310 nm. A and B, monitored at 363 nm; C and D, monitored at 450 nm. O,  $\tau_1$  (B and D);  $\Delta$ ,  $\tau_2$  (B and D);  $\square$ ,  $\tau_3$  (B and D).

function. As in the concentrated solutions, rising components were observed in the excimer emissions except for PACB11. For the monomer and excimer emissions for PACB $n$ , the temperature dependence of the lifetimes and the contribution of each component to the total fluorescence (judged by  $A_i\tau_i/\sum A_i\tau_i$ ) are shown in Figure 8. The monomer emissions were associated with fast-decaying components ( $\tau_1 = 30$ –100 ps), components with lifetimes  $\tau_2$  of 400–800 ps, and slowly-decaying components ( $\tau_3 = 2$ –5 ns). In the excimer emissions, we observed rising components with  $\tau_1$  of 200–500 ps. Furthermore, it is evident that the slowly-decaying components in the excimer emission ( $\tau_3 = 2$ –5 ns) correspond to those of the monomer emissions.

**Effects of Morphology of LC States on Fluorescence Behaviors.** Three-dimensional time-resolved fluorescence spectra in the wavelength range from 320 to 500 nm for PACB3 and PACB5 as typical examples, the third axes being the delay time after pulse excitation, are shown in Figure 9. In both spectra the emission due to excimer

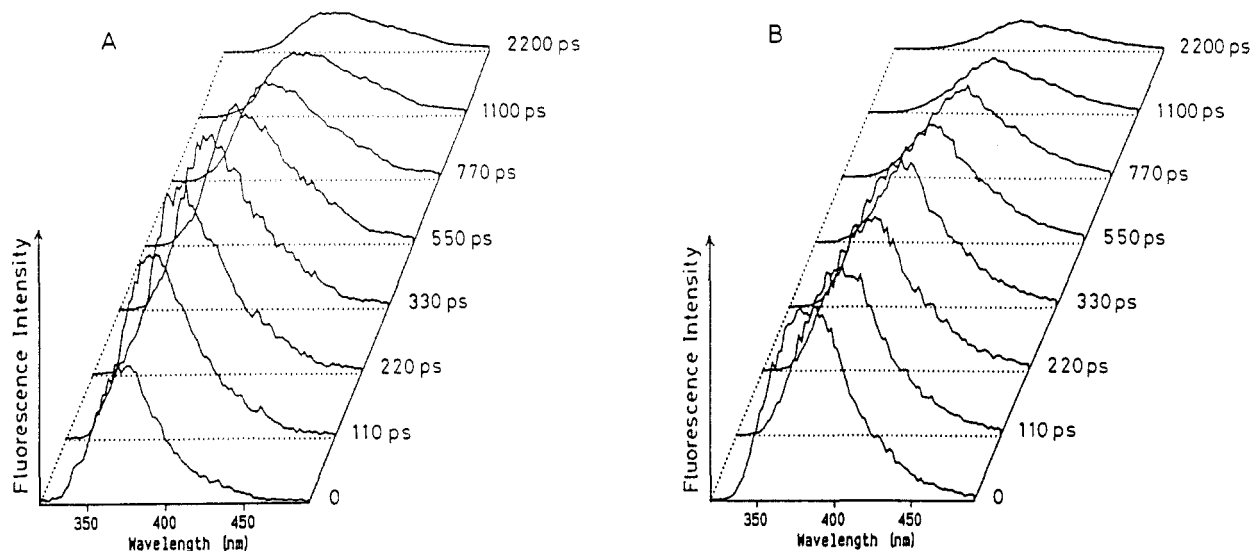


**Figure 9.** Three-dimensional time-resolved fluorescence spectra of neat PACB3 (A) and PACB5 (B) in the N state. Excitation was at 310 nm. The numbers in the figure denote the delay times after pulse excitation.

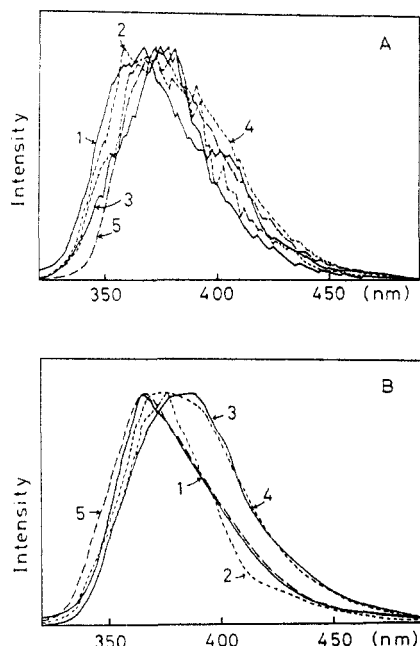


**Figure 10.** Time-resolved fluorescence spectra of PACB $n$  immediately after pulse excitation in the I state (A) and the LC state (B). 1, PACB2; 2, PACB3; 3, PACB5; 4, PACB6; 5, PACB11.

grows with time. However, one can see the distinction among spectra obtained at  $t = 0$  in the longer wavelength region. Emission spectra at  $t = 0$  in the I and LC phases of PACB $n$  are shown in Figure 10. Although some difference was seen in the I state, it became marked in the LC state. Specifically, PACB5 and PACB6 showed more red-shifted emission in the N state compared to the other fluorophores. This result implies that some fraction of the excimer originates directly from the excitation of the paired chromophores in the ground state as mentioned in the preceding section, and the CB mesogens are oriented closely in a regular manner in PACB5 and PACB6. Thus, they showed a high efficiency of excimer formation compared to the other PLCs as seen in Figure 6. The low efficiency of PACB2 and PACB3 in the neat film may be due to the strong coupling with the main chain. It is interesting to note the different behavior of the excimer formation of PACB3 in the neat film and in solution. In

the solution, because of the solvent molecules, the CB mesogens are highly mobile, while in the bulk they have only a restricted mobility owing to the influence of the main chain. The strong coupling of mesogens in the side chain with the main chain in PACB2 and PACB3 seems to have resulted in insufficient interaction between the CB chromophores in the LC state. On the other hand, for PACB11 showing a  $S_A$  phase, the crucial factor for the excimer formation is not the ground-state geometry but lateral diffusion of the mesogens. The layered structure of mesogens in the  $S_A$  phase is obviously favorable for excimer formation; however, the loss of mobility of the CB mesogens in the  $S_A$  phase due to its high viscosity will suppress the reorientation process and lead to the low efficiency of excimer formation.<sup>10</sup>

## References and Notes

- (1) Ciferri, A.; Krigbaum, W. R.; Meyer, R. B., Eds. *Polymer Liquid Crystals*; Academic Press: New York, 1982.
- (2) Kostromin, S. G.; Sinitzyn, V. V.; Talroze, R. V.; Shibaev, V. P.; Plate, N. A. *Makromol. Chem., Rapid Commun.* **1982**, *3*, 809.
- (3) Yamaguchi, T.; Asada, T.; Hayashi, H.; Nakamura, N. *Macromolecules* **1989**, *22*, 1141.
- (4) Plate, N. A.; Shibaev, V. P. *Comb-Shaped Polymers and Liquid Crystals*; Plenum Press: New York, 1987.
- (5) Cundall, R. B.; Dale, R. E. *Time-Resolved Fluorescence Spectroscopy in Biochemistry and Biology*; NATO Advanced Study Institute Series 69; Reidel: Dordrecht, The Netherlands, 1981.
- (6) Winnik, M. A. *Photophysics and Photochemical Tools in Polymer Science*; NATO Advanced Study Institute Series 182; Reidel: Dordrecht, The Netherlands, 1986.
- (7) Beddard, G. S.; West, M. A. *Fluorescence Probes*; Academic Press: New York, 1981.
- (8) Subramanian, R.; Patterson, L. K.; Vevanon, H. *Chem. Phys. Lett.* **1982**, *93*, 578.
- (9) Tamai, N.; Yamazaki, I.; Masuhara, H.; Mataga, N. *Chem. Phys. Lett.* **1984**, *104*, 485.
- (10) Ikeda, T.; Kurihara, S.; Tazuke, S. *J. Phys. Chem.* **1990**, *94*, 6550.
- (11) Shibaev, V. P.; Kostromin, S. G.; Plate, N. A. *Eur. Polym. J.* **1982**, *18*, 651.
- (12) Ikeda, T.; Lee, B.; Tazuke, S.; Takenaka, A. *J. Am. Chem. Soc.* **1990**, *112*, 4650.
- (13) Nakahira, T.; Maruyama, I.; Iwabuchi, S.; Kojima, K. *Makromol. Chem.* **1979**, *180*, 1853.
- (14) Leadbetter, A. J.; Frost, J. C.; Gaughan, J. P. *J. Phys. (Fr.)* **1979**, *40*, 375. Leadbetter, A. J.; Mehta, A. I. *Mol. Cryst. Liq. Cryst.* **1981**, *72*, 51.